AD-A193 165 PHYSICAL MECHANISMS IN SHOCK-INDUCED TURBULENT SEPARATED FLOW(U) TEXAS UNIV AT AUSTIN DEPT OF AEROSPACE ENGINEERING AND ENGINE.. D S DOLLING 1/1

UNCLASSIFIED 15 DEC 87 AFOSR-TR-88-0292 AFOSR-86-0112 F/G 20/4 NL

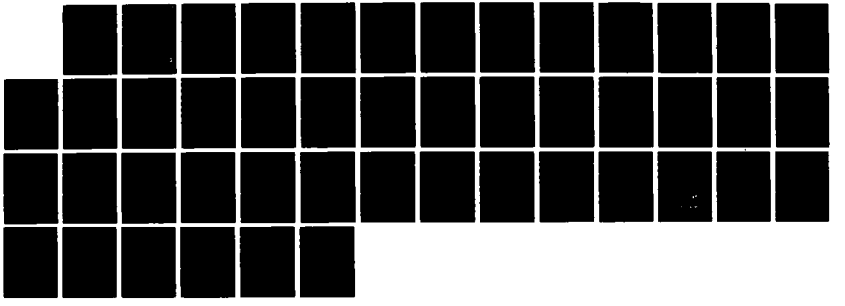

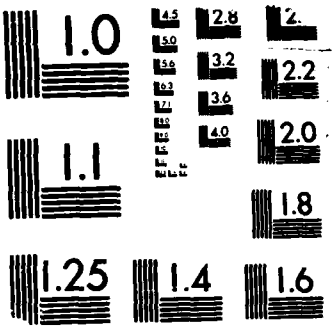

UNCLASSIFIED

2

REPORT DOCUMENTATION PAGE

DTIC FILE COPY

AD-A193 165

	1b. RESTRICTIVE MARKINGS
2b. DECLASSIFICATION / DOWNGRADING SCHEDULE	3. DISTRIBUTION / AVAILABILITY OF REPORT APPROVED FOR PUBLIC RELEASE DISTRIBUTION IS UNLIMITED
4. PERFORMING ORGANIZATION REPORT NUMBER(S)	5. MONITORING ORGANIZATION REPORT NUMBER(S) AFOSR-TR- 88-0292
6a. NAME OF PERFORMING ORGANIZATION UNIV TEXAS AT AUSTIN 6b. OFFICE SYMBOL (If applicable)	7a. NAME OF MONITORING ORGANIZATION AFOSR/NA
6c. ADDRESS (City, State, and ZIP Code) AUSTIN, TX 78712	7b. ADDRESS (City, State, and ZIP Code) BUILDING 410 BOLLING AFB, DC 20332-6448
8a. NAME OF FUNDING / SPONSORING ORGANIZATION AFOSR 8b. OFFICE SYMBOL (If applicable) NA	9. PROCUREMENT INSTRUMENT IDENTIFICATION NUMBER AFOSR-86-0112
8c. ADDRESS (City, State, and ZIP Code) BUILDING 410 BOLLING AFB, DC 20332-6448	10. SOURCE OF FUNDING NUMBERS PROGRAM ELEMENT NO. 61102F; PROJECT NO. 2307; TASK NO. A1; WORK UNIT ACCESSION NO.

11. TITLE (Include Security Classification)
(U) PHYSICAL MECHANISMS IN SHOCK-INDUCED TURBULENT SEPARATED FLOWS

12. PERSONAL AUTHOR(S)
D.S. DOLLING

13a. TYPE OF REPORT	13b. TIME COVERED	14. DATE OF REPORT (Year, Month, Day)	15. PAGE COUNT
ANNUAL	FROM 3/01/86 TO 11/30/87	12/15/87	44

16. SUPPLEMENTARY NOTATION

17. COSATI CODES			18. SUBJECT TERMS (Continue on reverse if necessary and identify by block number)
FIELD	GROUP	SUB-GROUP	SHOCK INDUCED SEPARATION, TURBULENT BOUNDARY LAYERS, REATTACHMENT

19. ABSTRACT (Continue on reverse if necessary and identify by block number)

It has been demonstrated that the flow downstream of the moving shock is separated and that the foot of the shock is effectively the instantaneous separation point. The shock induced turbulent separation is an intermittant process and the separation line indicated by surface tracer methods, such as kerosene-lampblack, is a downstream boundary of a region of intermittent separation.

DTIC ELECTE MAR 3 0 1988 S D

20. DISTRIBUTION / AVAILABILITY OF ABSTRACT	21. ABSTRACT SECURITY CLASSIFICATION
☐ UNCLASSIFIED/UNLIMITED ☒ SAME AS RPT. ☐ DTIC USERS	UNCLASSIFIED
22a. NAME OF RESPONSIBLE INDIVIDUAL JAMES M. MCMICHAEL	22b. TELEPHONE (Include Area Code) 202-767-4936
	22c. OFFICE SYMBOL AFOSR/NA

DD FORM 1473, 84 MAR — 83 APR edition may be used until exhausted. All other editions are obsolete.

SECURITY CLASSIFICATION OF THIS PAGE

UNCLASSIFIED

Rec 16 Feb 88

PHYSICAL MECHANISMS IN SHOCK-INDUCED TURBULENT SEPARATED FLOWS

Grant AFOSR-86-0112

AFOSR-TR- 88-0292

D. S. Dolling

Aerospace Engineering and Engineering Mechanics
The University of Texas at Austin
Austin, TX 78712

Technical Report
3/01/86 - 11/30/87

December 1987

Summary

The overall objective of this three-year program is to understand the physics of unsteady shock-induced turbulent boundary separation and reattachment. Specifically, this involves a study of the dynamics of the separation bubble in a nominally 2-D unswept compression ramp flowfield. The study is experimental and is being conducted in a Mach 5 blowdown wind-tunnel. Experiments have also been made in interactions generated by circular cylinders.

During the first twenty months of the program considerable progress towards these goals has been made. Using thin platinum films in a thermal-tuft mode and from cross-correlations of conditionally sampled wall pressure signals it has been demonstrated that the flow downstream of the moving shock is separated and that the foot of the shock is effectively the instantaneous separation point. Hence shock-induced turbulent separation is an intermittent process and the separation line indicated by such surface tracer methods as the well-known kerosene-lampblack method is a downstream boundary of a region of intermittent separation. From detailed measurements of the shock dynamics in 4 different cylinder interactions it has been proposed that pressure fluctuations in the separated shear layer drive the shock. An experiment to investigate this further is currently underway.

Other ongoing experiments discussed in this report which are being carried out in a compression ramp flow include (i) determination of instantaneous reattachment position, (ii) correlation of instantaneous separation and reattachment locations to determine bubble dynamics and (iii) measurement of spanwise separated flow structure.

Table of Contents

Section		Page
	Summary	(i)
1.	Research Schedule and Objectives	1
2.	Status of Research	1
	2.1 Background Information	1
	2.2 Research Findings	4
	2.3 Plans for Second Phase of Study	17
3.	Professional Personnel	19
4.	Publications	21
5.	Interactions	22
	Appendix A	23
	Figures	

1. Research Schedule and Objectives

The current program has been planned as a 3-year effort (3/1/86 through 2/28/89) and is split into two phases (3/1/86 through 10/31/87 and 11/1/87 through 2/28/89). This report outlines progress made in the first phase and details plans for the next phase.

The focus of this study is an experimental investigation of the separated flow dynamics of a nominally 2-D separated compression ramp flow through conditional sampling, space-time correlation and other analysis techniques. The objectives are to determine: a) How does separation occur (i.e., is the time-averaged model physically accurate)? b) Why is the separation process unsteady and what is the cause? c) Does the separation process and separated flow have an underlying 3-D structure? d) What is the structure and what is the cause? Through clarification of the structure and mechanisms in this type of flow a better fundamental understanding will be developed. It is hoped that this understanding will help answer the question of why numerical simulations do an inadequate job of predicting this type of flowfield, and contribute to improved modelling techniques.

2. Status of Research

2.1 Background Information

The special requirements of this study necessitated a large amount of preparatory work, both in terms of hardware and software. In the early stages of model design it became apparent that it would be necessary to station transducers anywhere in the interaction, upstream and downstream of the ramp corner. Being restricted to certain spanwise or streamwise stations would limit the measurements and hamper the analysis at a stage when modifications could not be easily accomplished. Consequently, a

decision was made to build a new test section, tailored to this experiment, but flexible enough for testing other geometries. The new section is made of Type 304 stainless steel, is about 1 foot long, and is installed between the existing nozzle/test section and the tunnel diffuser. Pertinent details are given below.

The test section and a partially exploded view showing the ramp assembly is sketched in Figs. 1a and 1b, respectively. The transducers can be located at any of 25 positions in a 3 in. diameter rotatable, flush plug or in plugs in the ramp. The ramp can be moved relative to the plug, and can also be slid in and out of the test surface, to vary transducer position relative to the corner line. The design was finalized in early September 1986 and drawings completed in October. Work in the machine shop started in December. The whole assembly is modular and consists of a significant number of precision parts with small tolerances. Consequently, construction was time-consuming and has taken about six man-months. The work was completed in June 1987.

To handle large volumes of data, the MassComp data acquisition system was upgraded. With grant funds and matching funds from the College of Engineering an additional 3 megabytes of high speed memory and an 80 megabyte Winchester disk drive have been installed. Grant and matching funds have also been used to purchase additional wide-band, high-gain amplifiers and filters to provide 8 channel capability.

During the period of model construction, a large fraction of the effort went into the development and validation of special data acquisition and analysis software. The codes include:

a) a "real-time" conditional sampling data acquisition code. One channel acts as a trigger to initiate data-taking on

the other channels (i.e., triggering occurs when a certain pressure level occurs, or when the shock is at a certain position). The system will take N simultaneous data points (at sampling rates up to 330 kHz) on M channels. N is user selectable while M can be up to 7. This code is needed for determining if specific flow structures correspond to specific conditions. Through ensemble averaging large numbers of the "same" events, an average structure corresponding to that event is deduced. Using different trigger settings an overall picture of the sequences of events in the flow can be built up.

b) a conditional sampling algorithm for use on multi-channel continuously sampled and recorded data. This code is for use in the intermittent region and isolates the shock motion from the turbulent boundary layer "noise". The pressure signal is converted into a square wave or "box-car" (Fig. 2). The development has not been a trivial task. Different algorithms using different methods have been thoroughly tested and the sensitivity to the thresholds examined. The end product is a reliable two threshold method. It was tested in Mach 5 cylinder-induced interactions and Mach 3 data taken earlier at Princeton. Results are presented in Ref. B1 (Section 4).

c) shock speed/direction calculation. Another set of codes takes the box-car representation of the pressure signals from b) and performs two analyses on them. First, space-time correlations are performed. The peaks at positive

and negative time delays provide information on the maximum shock speeds in the downstream and upstream directions respectively. Second, each passage of the shock over the transducer pair is examined individually and the upstream and downstream speeds calculated. Statistics can then be performed on the array of velocity pairs.

A substantial effort has gone into developing, writing and evaluating these codes. The codes were tested by taking data in interactions generated by circular cylinders since these experiments could be set up easily without the new test section. These preparatory efforts have proved to be detailed experiments in themselves, and have resulted in considerable insight into the validity of different conditional sampling algorithms and the driving mechanisms responsible for the separation shock unsteadiness. Some of the more important results from the first phase of the program are described below.

2.2 Research Findings

Several interrelated experiments have been conducted in this program. As noted earlier, while awaiting construction of the new test section and ramp model, experiments were made in 3-D interactions generated by circular cylinders. These experiments were carried out to develop and validate the instrumentation and software to be used in the ramp study. However, since the shock-induced turbulent boundary layer separation process in both types of flows has many qualitative and quantitative similarities, they have proven invaluable in shedding new light on the shock dynamics and the possible driving mechanism.

Since June 1987 the new test section and ramp models have been available and two experiments have been conducted. A third is currently

in progress. All of these experiments were performed in the 7 in. x 6 in. blowdown tunnel at a nominal freestream Mach number of 5. In all cases the turbulent boundary layers developed naturally. No trips were used.

The experiments, their objectives, and a brief summary of results are presented below. The work is described in the order in which it was carried out.

a) Experiment: Use of platinum thin films as thermal tufts to detect instantaneous flow direction adjacent the surface.

Objective(s): To determine the physical meaning of separation lines as indicated by surface tracer techniques. The latter provide well defined, repeatable "separation" lines and are widely used to evaluate the capabilities of numerical simulations, yet what they represent physically in an unsteady flow is not clear.

Results: The first phase of the work employed a single detector film operated at low overheat ratio and a single continuously heated film downstream of it (Fig. 3a). The arrangement was located in the region of separation shock oscillation, upstream of the separation location as indicated by surface traces. The tests were made in the interaction generated by a circular cylinder.

It was hypothesized that as the shock moved forward, then the heat carried upstream by the backflow passing over the heated film would increase the detector film resistance with accompanying voltage change. Analysis of the instantaneous detector film voltage level would therefore indicate flow direction and hence indicate if the flow was separated downstream of the instantaneous shock position.

Unfortunately, it was found with this arrangement that the sensitivity of the detector film was inadequate to observe unambiguously the motion of the instantaneous separation point. However, through conditional analysis of the detector film signals it was inferred that the flow downstream of the moving shock wave was separated and that the instantaneous separation point is at the foot of the moving shock wave. This was done by calculating the power spectral density of the voltage fluctuations of the parts of the signal corresponding to flow upstream and downstream of the shock wave and showing that the spectra were the same as those in the undisturbed incoming turbulent boundary layer and in the separated flow respectively. Hence it was inferred that the separation line indicated by surface tracers is a downstream boundary of a region of intermittent separation; it is not a mean separation line. A simple physical model explaining this result, is reported in Ref. A1 (Section 4), which also describes the work in further detail.

This inference has since been proven using two techniques. One is an improved thin film technique, the other is a novel method which deduces if the flow is separated from fluctuating wall pressures. The latter is discussed separately under d) below. The improved film technique uses an array of heated films upstream of the detector film, and a cooled surface (internal circulation of methanol cooled by dry ice) downstream of the detector (Fig. 3b). In this way, as the flow adjacent the surface changes direction, the temperature change felt by the detector film is larger and measurable. Details of the method and results are provided in Ref. D3 (Section 3).

However for many applications, particularly where space constraints exist, this method may not be practical and use of pressure

transducers, as described in d) below is preferable.

b) Experiment: Measurement of fluctuating wall pressures under oscillating separation shock wave in separated 3-D shock wave turbulent boundary layers induced by semi-infinite circular cylinders.

Objective(s): (i) develop conditional sampling algorithm capable of discriminating consistently between shock-induced pressure fluctuations and those due to turbulence. This is necessary to isolate the shock motion and analyze it independently of the undisturbed and disturbed boundary layer components of the signal. The accuracy and reliability of this algorithm is critical since many of the parameters of importance (see (ii) below) must be deduced from it.

(ii) examine influence of cylinder diameter and incoming boundary layer properties on the shock dynamics (i.e., frequency and period distributions, power spectral density, and shock speeds in upstream and downstream directions). Through examination of these quantities and their variation with the parameters varied it was hoped that new light could be shed on the mechanism driving the shock motion.

Results: These experiments have been reported in detail in Refs. B1, B2 and C1 (Section 4). Only a very brief summary is presented below.

Two cylinders of diameter, D, 1.27 and 1.91 cm were tested in the tunnel floor boundary layer and in the boundary layer which developed on a full span flat plate test surface ($\delta \cong .63$ in. and .25 in. respectively). Wall pressure fluctuations under the oscillating separation shock wave were recorded on two channels simultaneously at sampling rates of up to 500 kHz/channel.

A detailed study was made to develop a reliable and accurate conditional sampling algorithm. A 2-threshold method was developed and sensitivity studies carried out. This is reported in detail in Ref. B1. In brief, the algorithm isolates the shock component of the wall pressure signal and converts the raw pressure signal into a variable frequency, fixed amplitude (unity) box-car function as shown in Fig. 2. Time-series analysis techniques and custom-tailored 'timing' codes were then used to analyze the box car signals.

Both D and δ influence the shock dynamics. However the mean frequency of the shock motion $\bar{f}$ (defined in Fig. 2) and zero crossing frequency, f_c, (defined in Fig. 2) are very low compared to the typical large eddy frequency in the incoming boundary layer. Probability distributions of the shock period, T_i, and frequency, f_i, are shown in Figures 4 and 5 respectively. The zero crossing frequencies as a function of intermittency are shown in Fig. 6 and are also low. Although the range of shock frequencies extends up to 10 kHz, values less than 2kHz are much more probable.

Shock speeds (typical histograms are shown in Figure 7) are also extremely low with mean values of about 0.06 - 0.07 U_{oo} and maximum values of about 0.2 - 0.3 U_{oo}. They are about the same in both upstream and downstream directions, with some evidence that the latter are slightly

higher. The speeds are independent of location in the intermittent region --- a composite plot of histograms of the shock speeds in the upstream and downstream directions for several intermittencies (i.e., at several locations in the intermittent region) shows this quite clearly (Fig. 8).

It has been suggested by Andreopoulos and Muck, who made measurements at Mach 3 in the intermittent region of separated compression ramp interactions, that "turbulence of the incoming boundary layer is largely responsible for the shock wave motion." This conclusion stemmed from the observations that the shock zero crossing frequency was the same order as the estimated bursting frequency in the incoming boundary layer and that shock velocities were of the same order as velocity fluctuations in the flow field. However, it is not necessary that the shock motion be connected with transport phenomena; the shock is an interface and its propagation speed depends on the pressures P_1 and P_2 in the upstream and downstream regions respectively. Analytically, the shock velocity, W, in the streamwise direction can be written as

$$W = \frac{a_1}{\sin\beta}\left[\frac{\gamma+1}{2\gamma}(P_2/P_1 - 1) + 1\right]^{1/2}$$

where a_1 is the speed of sound in the upstream region, β is the shock angle and γ is the ratio of specific heats. The measured separation pressure ratio is about 1.9 which for an incoming Mach number of 4.9 corresponds to a shock angle of about 15.7^{o}. These values give W = 740 m/s, the free-stream velocity. In the simplest possible case with a_1, β, γ and P_1 fixed, W will depend only on changes in P_2. The data show that P_2 varies approximately ± 4200 Nm^{-2} (± 0.6 psi) about its mean value of 1.9 P_{oo} with

smaller amplitudes more probable. Table 1 below shows the change in W/U_∞ from the equilibrium value of unity obtained by varying the value of P_2 by $\pm n\sigma_{p_\omega}$ where $1 \leq n \leq 3$. Positive increments in P_2 generate an increase in W (i.e. upstream excursion of shock) and vice-versa.

TABLE 1
ESTIMATED SHOCK SPEEDS

	$\Delta W/U_\infty$	
	Upstream	Downstream
$P_2 \pm 1\sigma_{P_w}$	0.072	0.065
$P_2 \pm 2\sigma_{P_w}$	0.140	0.166
$P_3 \pm 3\sigma_{P_w}$	0.206	≈0.249

Comparison of the tabulated results with the data suggests a correlation. Except in the first case (due to the non-linearity of the equation) the calculated downstream speed is of order 10-20% higher than the upstream value, a feature observed experimentally. Second, since the amplitude distribution of the pressure fluctuations is essentially Gaussian, a larger fraction of the fluctuations will have smaller amplitudes than larger amplitudes. This would bias the shock speed distributions to low values of U_∞, also a feature seen experimentally. Third, the predicted maximum speeds, which would correspond to fluctuations with amplitudes of $\pm 3\sigma_{p_\omega}$ correlate well with the measured ones. The very small fraction of shock speeds found at $0.5\ U_\infty$ in Figure 7 is probably a result of the conditional sampling algorithm.

At this stage, in the absence of confirming data, the above idea must be viewed with caution. However, since it does reproduce several of the observed experimental features it warrants further investigation. This requires an experiment using several pressure transducers in which pressure fluctuations at the upstream edge of the separated flow are correlated with shock direction and speed. This experiment is currently underway.

c) Experiment: Exploratory study of spanwise properties of the unsteady separation shock wave in a separated, unswept compression ramp flowfield.

Objective(s): (i) Time-averaged measuring techniques such as surface tracers have shown that nominally 2-D separated compression ramp flows actually have a well defined 3-D spanwise vortex structure (Fig. 9). The structure and dynamics of the separation shock system which generates this result is largely unknown. Before investigating the dynamics of the separation bubble (the primary objective of this program) which involves monitoring in real-time the instantaneous streamwise location of the separation and reattachment points it is necessary to understand how the shock structure varies spanwise.

Results: To date, fluctuating wall pressure measurements have been taken along a spanwise line in the intermittent region upstream of the separation line. The experiments on this first phase are completed and the analysis is almost completed. Standard time-series analysis techniques and a technique which performs direct statistics on the time delay between shock passages on two simultaneously sampled signals have been used. Due to the difficulties of interpreting the results a definitive statement about the physical characteristics of the shock motion cannot yet be made.

Both variable and fixed transducer spacings were used in making spanwise measurements in the intermittent region. The first set of tests involved fixing a reference transducer near the center-line of the tunnel and moving a second transducer away from it in increments of 0.115 in. The reference transducer was used to ensure that if any gross flowfield changes occurred, they would be known. A total span of 2.76 in. ($3.94\,\delta_o$) was covered. Since the reference transducer was fixed, the largest spanwise separation was 1.38 in. ($1.97\,\delta_o$). In the second set of tests, two transducers were placed 0.115 in. ($0.115\,\delta_o$) apart. This arrangement was then placed at several spanwise locations.

To aid in the analysis of the spanwise results, "statistically independent runs" (SIRs) were created to act as references for comparison with the actual data. The SIRs were generated as follows. The last 2 records (2048 points) of one channel of data, of the 2 channel file, were transferred to the beginning of the channel and the rest of the data was shifted forward 2048 points. This shifted the 2 channels of simultaneously sampled signals by 6144 μs (chosen because very few shock periods of over 6000 μs occur). Analysis verified that the 2 signals were indeed statistically independent. The coherence function was essentially zero for all frequencies and the cross-correlation showed low-level, broad-band correlation characteristic of random noise.

The two-threshold conditional analysis algorithm was used to separate pressure fluctuations due to shock motion from fluctuations associated with the upstream and downstream boundary layers. Two parameters are calculated directly from the converted signal. The first is

the intermittency, γ, which is essentially the number of 1's in the converted signal divided by the total number of points per channel. A second parameter, co-intermittency, γ', is defined as the fraction of time both channels are disturbed by the shock wave at the same time. On the converted signals, this is the fraction of time the two channels share time in the "on" state.

It is necessary to take into account the spanwise variations in γ to extract useful information from the distributions of γ and γ'. Those variations in the mean flowfield are taken into account by subtracting the intermittency calculated at the reference position γ_{ref} for each run. Similarly, variations in γ' are accounted for by subtracting out γ'_{th}, the theoretical minimum co-intermittency. γ'_{th} is that value for two statistically independent signals, and is simply the product of the individual intermittencies. Distributions of $[\gamma - \gamma_{ref}]$ and $[\gamma' - \gamma'_{th}]$ vs. ε the spanwise displacement from the reference point normalized by δ_o, are shown in Figure 10. The $[\gamma' - \gamma'_{th}]$ distribution decreases rapidly from its theoretical maximum $(0.61 - 0.61^2)$ with increasing separation, then tails off at values just above the limit of SIRs.

Figure 11 shows the maximum cross-correlation coefficient, $R_{pp,max}$, vs. ε with $R_{pp,max}$ of the SIRs drawn in for reference. The behavior of this curve is similar to that of $[\gamma' - \gamma'_{th}]$. The curve decays rapidly with increasing separation and slowly approaches $R_{pp,max}$ of the SIRs.

The coherence function for several spanwise separations is shown in Figure 12. The two upper data sets indicate broad-band coherence, with the low frequencies of shock motion highly coherent. Coherence drops quickly as lateral spacing ε increases. The frequency at which the coherence drops to 0 also decreases with increasing separation, meaning

that as ϵ increases, only progressively lower frequency, higher amplitude shock passages remain coherent. The coherence plots for $\epsilon = \pm 1.97$ show that it is only the lowest frequency shock motions which cause $R_{pp,max}$ and the co-intermittency to remain above the statistically independent limit.

A "timing" code was also developed to gain a better understanding of the shock dynamics. This timing code is discussed in Appendix A. Figure 13 shows the total number of rise and fall events occurring within a ± 1200 μs window. The reference line shown is the average number of events for the SIRs. This plot shows trends similar to Figs. 10 and 11, except that the decay is more rapid for small separations. The theoretical maximum at $\epsilon = 0$ is about 1200, the number of shock passages, but for clarity it is not shown.

The mean delay time for each type of event (R_1,F_1,R_2,F_2) is plotted vs. ϵ in Figure 14. The shape of the curves is the inverse of those of Figs. 10, 11 and 12. The mean delay times for the four types of events are nearly the same and increase linearly with separation to about $\epsilon = \pm 0.75$ where the distributions begin to asymptote to some value in the range of the mean delays of the SIRs. For all $\epsilon > 0$, the delays are close in value and asymptote to within several percent of the SIR mean delay (except for $\epsilon = 1.97$, for which there was a gross change in the mean flowfield).

All of the curves shown are symmetric about the reference point, which is 0.08 δ_o to the right of the tunnel centerline. If the shock wave undergoes random rippling then the reference should not be a special location and results would be similar for a reference placed at any point across the span. To verify this and to investigate the small scale shock structure further, 6 sets of measurements on 2 adjacent transducers were

made across a span of $1\delta_o$. The mean delays and numbers of events were almost exactly the same for all 6 runs. This confirms the apparent random nature of the rippling and shows that the reference position chosen was not a unique point in the interaction. Currently further analysis is underway and consequently final conclusions about the shock structure have not yet been drawn.

d) Experiment: Detection of instantaneous separation point through cross-correlations of conditionally sampled pressure signals.

Objective(s): The objectives of this experiment were essentially the same as those described under a) above for the thin film thermal tuft studies. Since pressure transducers are much more easily installed and used than the film technique a study has been made to determine: (i) If they can be used to detect separated flow, (ii) then, having shown (i) to be the case is the flow downstream of the shock separated (i.e., does the instantaneous shock foot represent the instantaneous separation location?)

Results: The basic approach is best explained with the aid of Figure 15. In the experiment, data are recorded simultaneously on channels 1 and 2. The proof that the flow downstream of the shock is separated is based on the following. Those portions of the signal that correspond to flow downstream of the shock were first extracted from the signal (i.e., time spans AA' and BB' in pressure-time traces 1 and 2 respectively). Cross

correlations were then made of N blocks of BB' with AA'. N typically varied up to 700. The resulting cross-correlations showed two peaks; one at positive τ and one at negative τ (Fig. 16). These cross-correlations have the same features, with maxima at the same values of τ, as cross correlations made downstream of 'S', the separation line indicated by surface tracers. Physically, the maxima at positive τ corresponds to large-scale eddies in the separated shear layer travelling downstream; maxima at negative τ corresponds to upstream convection (i.e., upstream moving separated flow adjacent the wall). Broadband convection velocities calculated from the values of τ at the maxima and the transducer spacing are what would be expected (namely about 0.5 U_{oo} downstream and about 0.2 U_{oo} upstream).

These results show that (i) the flow downstream of the instantaneous shock location is separated, (ii) shock-induced turbulent separation is an intermittent process, and (iii) the separation line from surface tracers is the downstream boundary of a region of intermittent separation.

e) Experiment: Investigation of driving mechanism of shock oscillation in separated compression ramp flows.

Objective(s): This experiment is an outgrowth of the speculation of the previous two sections. The objective is to identify the mechanism driving the separation shock motion. Since the separation shock foot is the instantaneous

separation point then identifying the mechanism driving the motion is an important, if not the most important, key to understanding the bubble dynamics.

Results: This experiment is currently underway and employs conditional sampling of the pressure signals in the intermittent region and under the separated shear layer. From the former, the instantaneous shock position and direction of motion can be obtained. These will be correlated with the large amplitude pressure fluctuations in the shear layer. The objective is to determine if rising pressure in the shear layer is associated with upstream motion of the shock and vice-versa. This is a fairly simple idea in principle but is not straightforward to code in a foolproof fashion. Currently results are not available.

2.3 Plans for Second Phase of Study

Three experiments are planned in the second phase. They will all be made in the compression ramp flowfield.

(i) experiment e) above, to determine the driving mechanism of the shock motion, is underway and will be continued.

(ii) measurement of instantaneous reattachment position on the compression ramp face. This will be attempted using the signals from pressure transducers oriented streamwise in the vicinity of reattachment. The technique planned involves the calculation of cross-correlations; peaks at negative time delay indicating the presence of upstream flow. These cross correlations will be calculated at extremely short intervals. If success-

ful, the technique will not be able to follow the reattachment location in real-time but it will be able to bracket its position (i.e., between transducers) and update this several thousand times per second.

(iii) correlate the instantaneous separation and reattachment locations and determine the bubble dynamics.

3. Personnel Supported by and/or Working on Project

A) Salaried Employees:

- Dr. D. S. Dolling is the PI and was supported 1 1/2 months per annum (summer 1986 and 1987).
- Walter Sauriol, machinist; 2 months support for test section construction. Remaining costs were borne by the department.

B) Graduate Students

J. C. Narlo, M. Erengil, D. Barnette and H. Baade, graduate research assistants, have received direct support from the grant. Mr. Baade has also received support from CEHTR (Center of Excellence in Hypersonics Training and Research sponsored by NASA, AFOSR AND ONR). J. C. Narlo, H. Baade and D. Barnette have now graduated (Section 8c). Mr. Erengil will complete his MS thesis by May 1988.

C) Additional Personnel Working on Project or Related Aspects

- R. Nordyke, graduate research assistant, has been supported through CEHTR and has been involved in a study of the spanwise character of the shock oscillation in the compression ramp flow.
- Douglas Smith is an Air Force officer who was on leave to obtain an MS degree and was self-supporting. He has carried out experiments using cylinders on the tunnel floor in support of code development.

D) Advanced Degrees Awarded

- Narlo, J. C., II (MS Thesis, completed Dec. 1986) "Experimental Investigation of the Driving Mechanisms of Separation Shock Wave Motion in Interactive Flows".
- H. Baade (MS Thesis, completed May 1987) "Time Series Analysis of

Separation Shock-Induced Pressure Fluctuations in Turbulent Interactive Flows".

4. Publications in Refereed Technical Journals

A) Published or Accepted for Publication

1) R. A. Gramann and D. S. Dolling "Interpretation of Separation Lines from Surface Tracers in a Shock-Induced Turbulent Flow" (accepted by AIAA Jnl).

2) D. S. Dolling and J. P. Dussauge "Fluctuating Wall Pressure Measurements" (to be published in a "Survey of Measurements and Measuring Techniques in Rapidly Distorted Compressible Turbulent Boundary Layers" in Agardograph series, Spring '88.)

B) Papers Under Review

1) D. S. Dolling and L. Brusniak "Separation Shock Motion in Blunt and Sharp Fin, Cylinder and Compression Ramp Flows" (submitted to AIAA Jnl).

2) D. S. Dolling and D. R. Smith "Unsteady Shock-Induced Turbulent Separation in Mach 5 Cylinder Interactions" (submitted to Jnl of Spacecraft & Rockets).

C) In Preparation

1) D. S. Dolling and H. Baade "Separation Shock Wave Dynamics in Mach 5 Turbulent Flow" (to be submitted to Journal of Fluid Mechanics).

2) R. Gramann, D. S. Dolling and D. Barnette "Physics of Shock-Induced Turbulent Boundary Layer Separation" (to be submitted to AIAA Jnl).

5. Interactions

A) Papers Presented at Meetings

1) D. S. Dolling and J. C. Narlo, II "Driving Mechanisms of Separation Shock Motion in Hypersonic Interactive Flow" Paper #7, Agard Conference on "Aerodynamics of Hypersonic Lifting Vehicles" April 1987 (Bristol, UK), Agard CP 428, 1987.

2) D. S. Dolling and L. Brusniak "Separation Shock Motion in Blunt and Sharp Fin, Cylinder and Compression Ramp Flows" Paper #87-1368, AIAA Fluid Dynamics, Plasma Dynamics and Lasers Conference, June 1987, Hawaii.

3) In preparation for 1st National Fluid Mechanics Congress, July 1988. R. Nordyke and D. S. Dolling "Spanwise Properties of the Unsteady Separation Shock Wave in a Mach 5 Unswept Compression Ramp Flow".

Appendix A

Shock Timing

At a fixed point in the intermittent region, two distinct events due to shock wave motion are possible. The first corresponds to motion upstream resulting in a rapid pressure rise. The second is a sharp decrease in pressure, to the level of the incoming boundary layer, which corresponds to passage of the shock downstream. On a single channel of the conditioned wall pressure signal at that point, the upstream motion is represented as a change from 0 to 1, a "rise event", and the downstream passage is represented as a change from 1 to 0, a "fall" event.

Two simultaneously sampled signals from transducers placed spanwise in a 3-D interaction present a complex situation. Shock passage events may not occur at the same time. Complete events (rise and fall) may be sequential, nested or may occur only on one channel; the signals may rise or fall at the same time; and, several rise and fall events may occur on one signal while only a few occur on the other during the same time span. Combined, there are more than twenty possible types of shock passage events on the two signals. The problem is made easier if individual rise and fall events are treated separately. However, all information about nested and sequential events is lost.

The algorithm developed for this study determines the time delays between rise and fall events on two channels of conditioned wall pressure signals for which the events share some common time in the "on" state. The "shared-time-up" criterion virtually assures that the events on the two channels correspond to the same instantaneous shock motion for two transducers, at least at small separations. However, a certain number of events fulfilling the shared-time-up criterion would be expected even

on uncorrelated, statistically independent signals. Thus, the time delay results must be interpreted with caution.

For calculation of the time delays, both channels of data were incremented by the same counter to eliminate any out-of-sequence problems. As the datafiles are sequenced through, each data point is subtracted from its successor. In this way, a difference of 1 corresponds to a rise event and a difference of -1 represents a fall event. At the beginning of the code, a time window is set. Events on one channel corresponding to rise or fall events at an earlier time on the other must occur within this window to be analyzed. Assuming both channels start at zero, the algorithm proceeds as follows. If a rise event occurs on Channel 2 (Ch1) a timing counter is initialized and a shock counter is incremented. For each time interval ($1/f_s$) that Ch1 remains up, the timing counter is incremented until one of two events occurs: a rise event on Channel 2 (Ch2) or a time elapse greater than the predetermined window. When Ch2 rises within the time window, the number of time intervals between rise events is written to a 4 x n array corresponding to the type of event and channel it first occurred on (for example, rise on Ch1 or fall on Ch2). Statistics on the four classes (2 events x 2 channels) of delay time are calculated from this array. The types of events will be referred to as R1 for rise events occurring on Ch1 first and so on for F1, R2 and F2.

A histogram of the discrete delay times is also calculated. The window width chosen for the time delay calculation determines the range of the distribution. For simplicity, both rise distributions and both fall distributions are plotted on the same axes. Channel 1 was chosen as the reference signal and delays for events which occurred on Ch1 first were

determined using a positive increment and assigned positive values while the opposite is true for events occurring first on Ch2.

Many shock passage events are not classified as either rise or fall events as defined above. Important information about shock motion may be obtained from these "non-events" however. Non-events identified and counted are: complete (rise and fall) shock passages on one channel without an event on the other; times when signals rose or fell together; and times when a signal either rose or fell without a corresponding event occurring on the other channel within the time window.

The timing characteristics of shock passages on one channel are essential to analysis of the results of the time delay algorithm. Using similar event-detection logic, the time between successive rise events, shock period T_i, on each individual channel is calculated. The periods are summed and divided by the number of shock events, $\underline{n}$, to obtain the mean shock period, T. The time between successive rise and fall events on a single channel, shock persistence, P, is an important parameter due to the shared-time-up criterion of the time delay calculation.

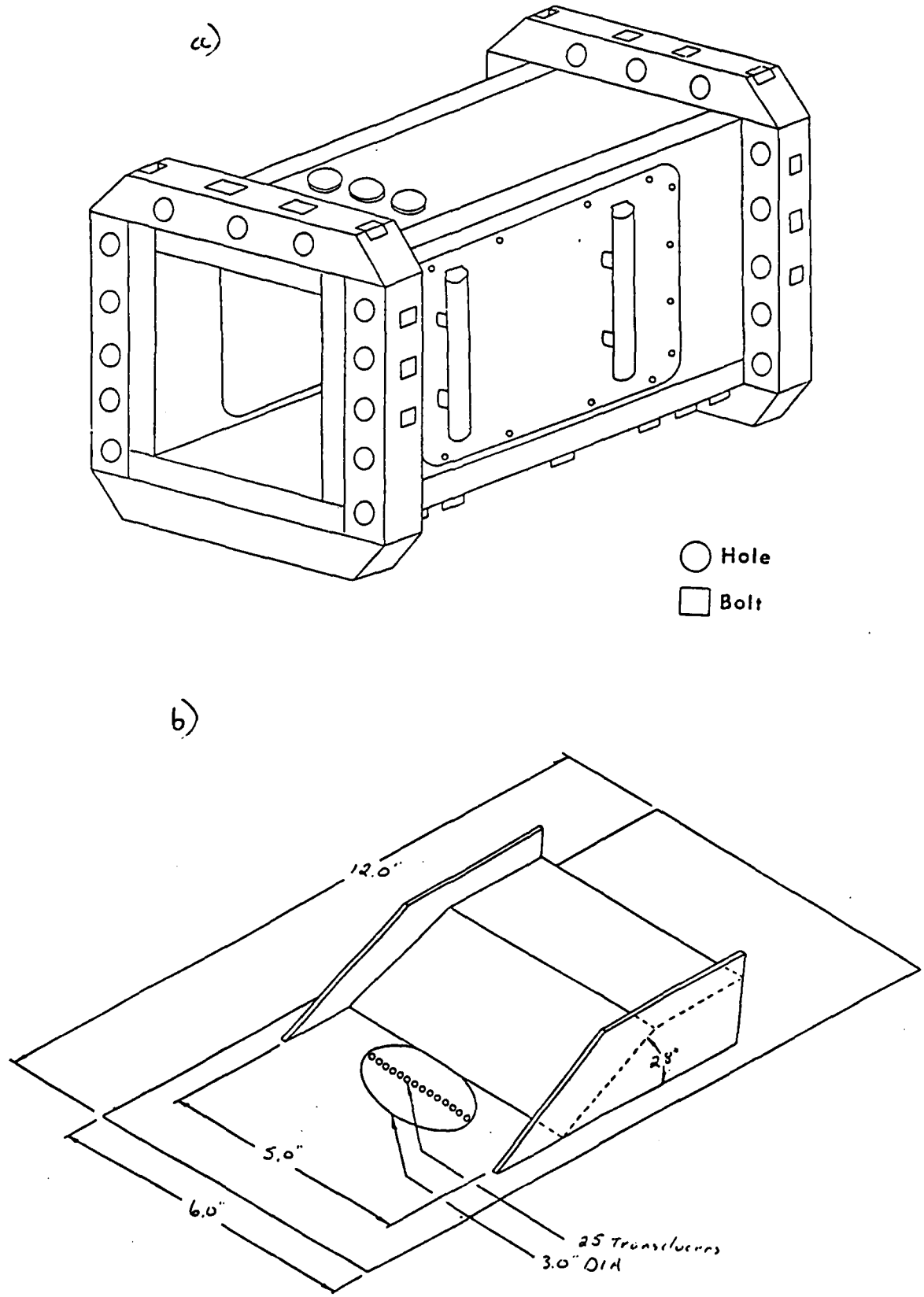

Fig. 1 Test Section and Model

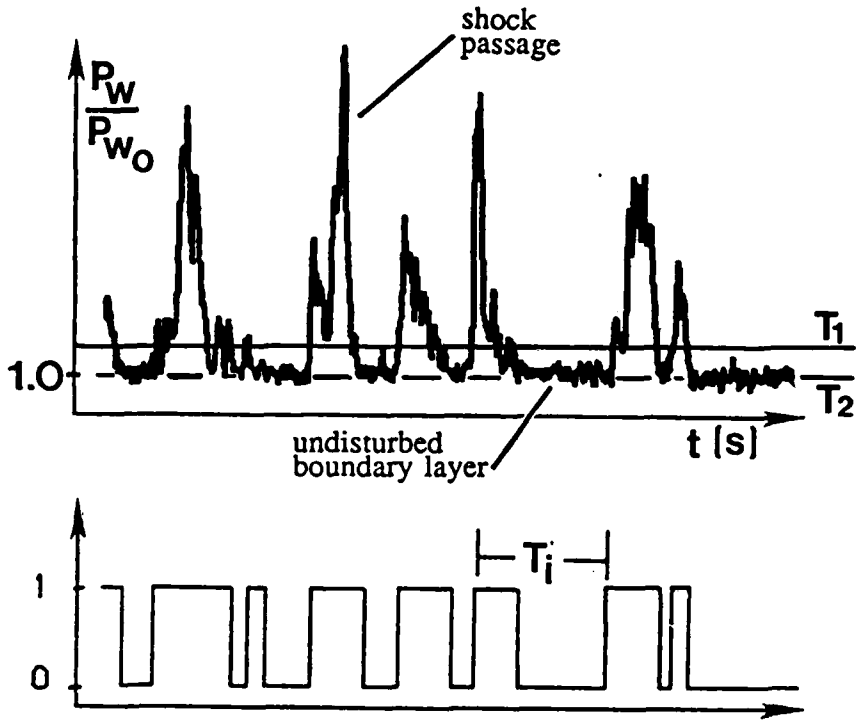

T_i = shock period (above)

$f_i = 1 / T_i$

$$f_c = 1 / T_m = 1 / \frac{1}{N} \sum_{i=1}^{N} T_i$$

$$\bar{f} = 1 / \frac{1}{N} \sum_{i=1}^{N} f_i = 1 / \frac{1}{N} \sum_{i=1}^{N} 1/T_i$$

[Note: $\bar{f} \neq f_c$]

Figure 2. Wall Pressure Signal near Separation and Conversion to Box-Car Signal with Period T_i and Amplitude Unity

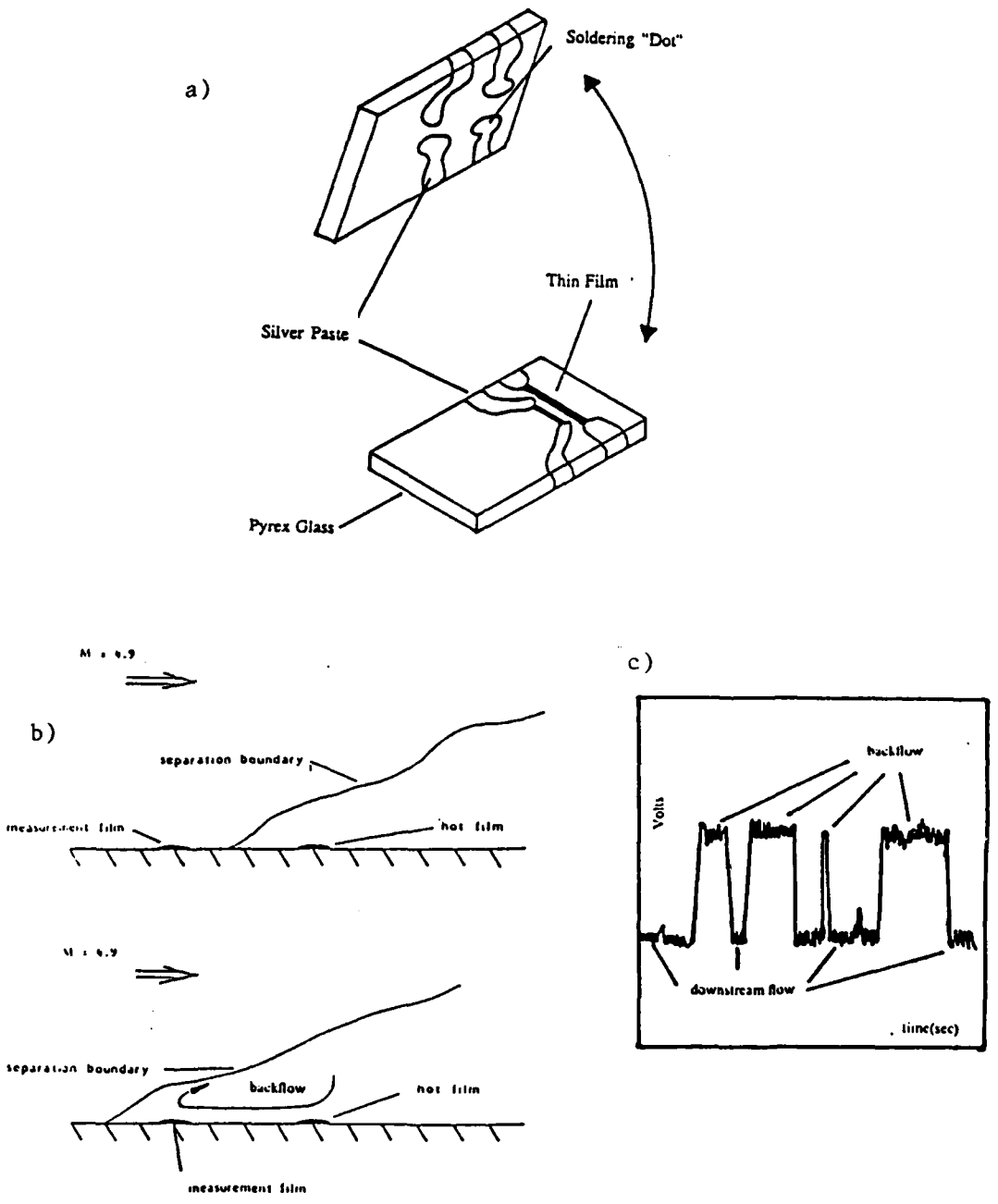

Figure 3. Initial Hot Film Arrangement. a) Heated and Detector Films, b) Principle of Operation, c) Anticipated (Idealized) Voltage Output

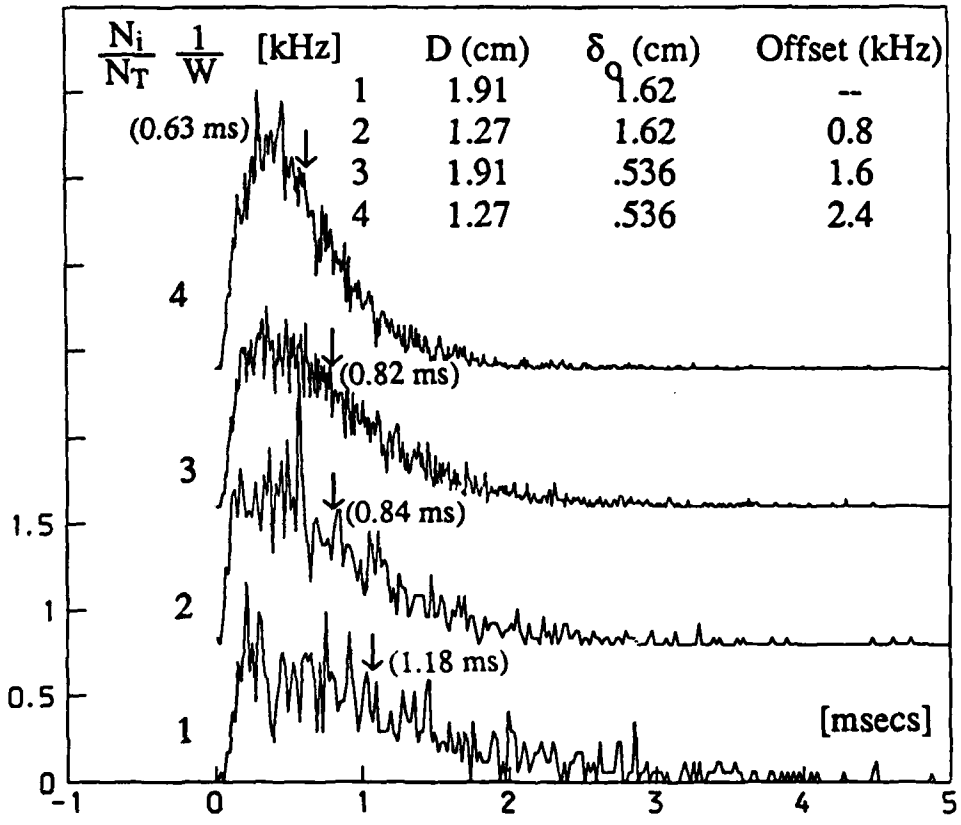

Figure 4. Probability Density Distributions of Shock Periods in Cylinder-Induced Separated Flows (Mean Period Indicated by Arrow)

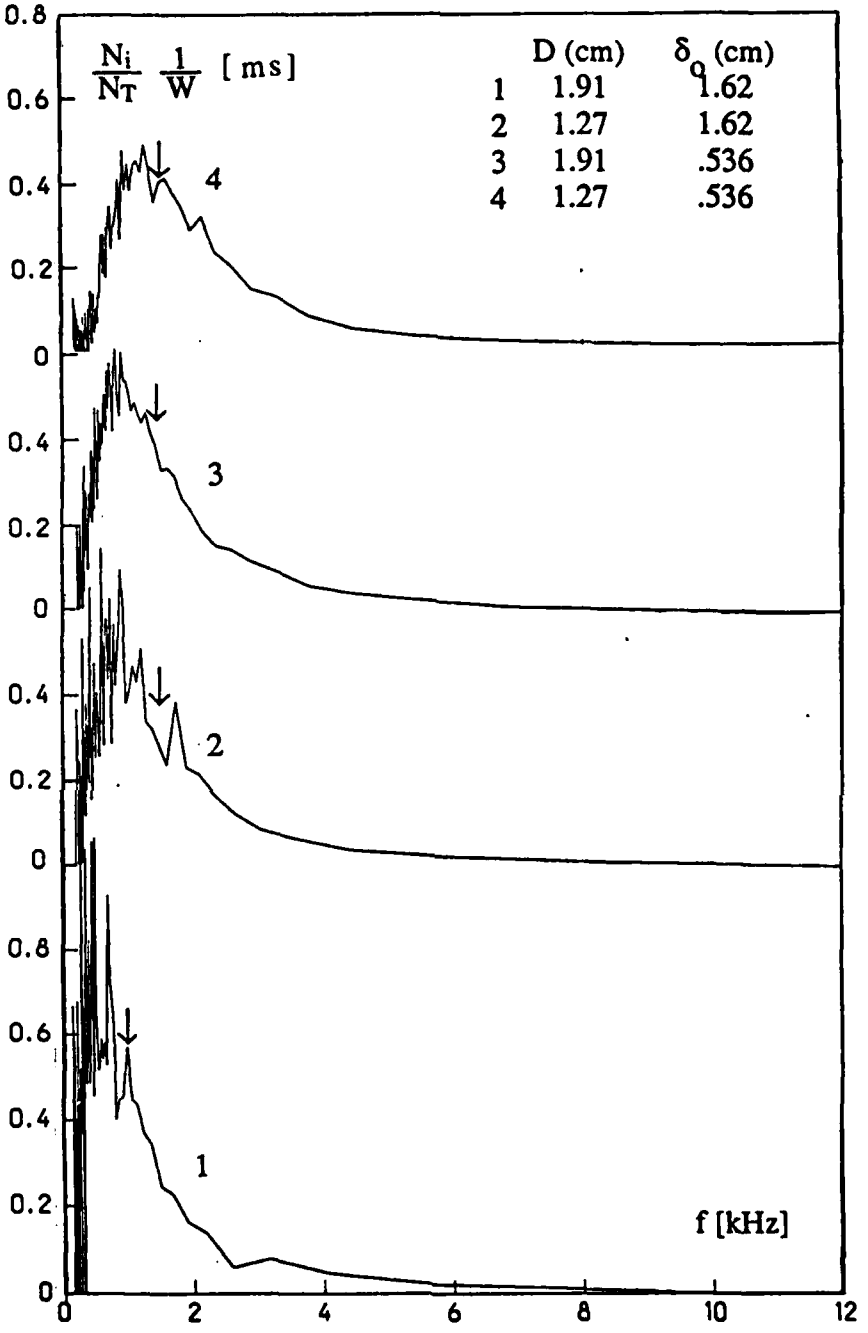

Figure 5. Probability Distributions of Shock Frequencies in Cylinder-Induced Separated Flows (Mean Values Indicated by Arrows)

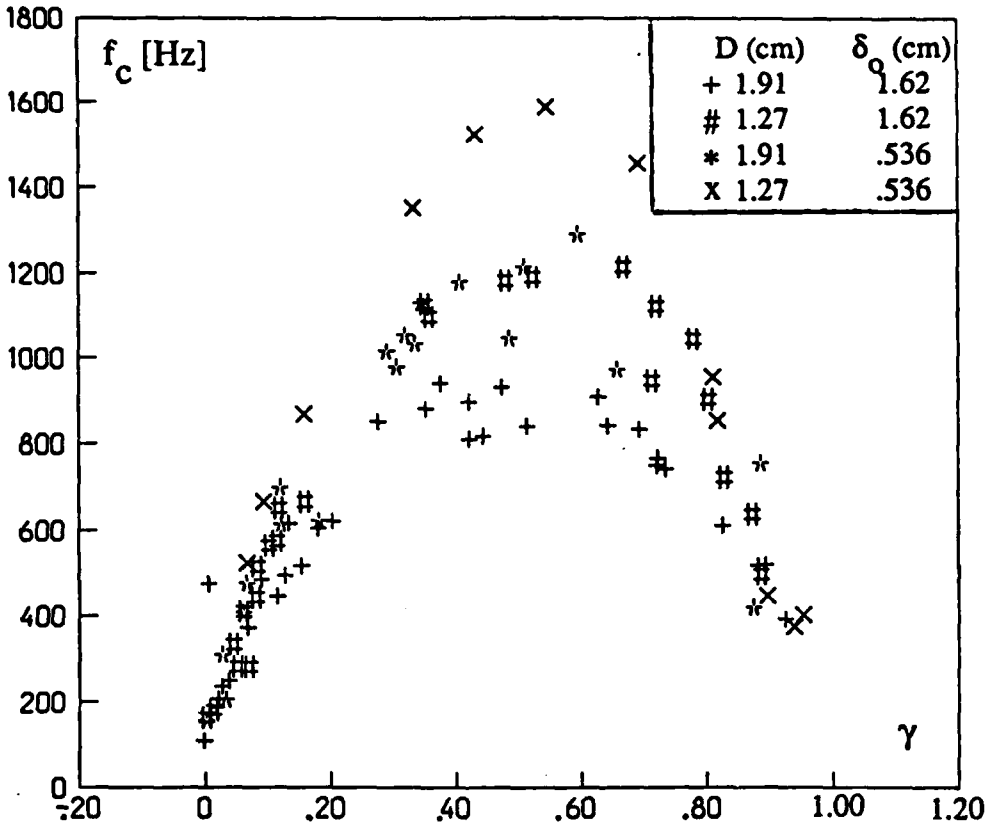

Figure 6. Distributions of the Zero Crossing Frequency as a Function of Intermittency for Cylinder Induced Separated Flows

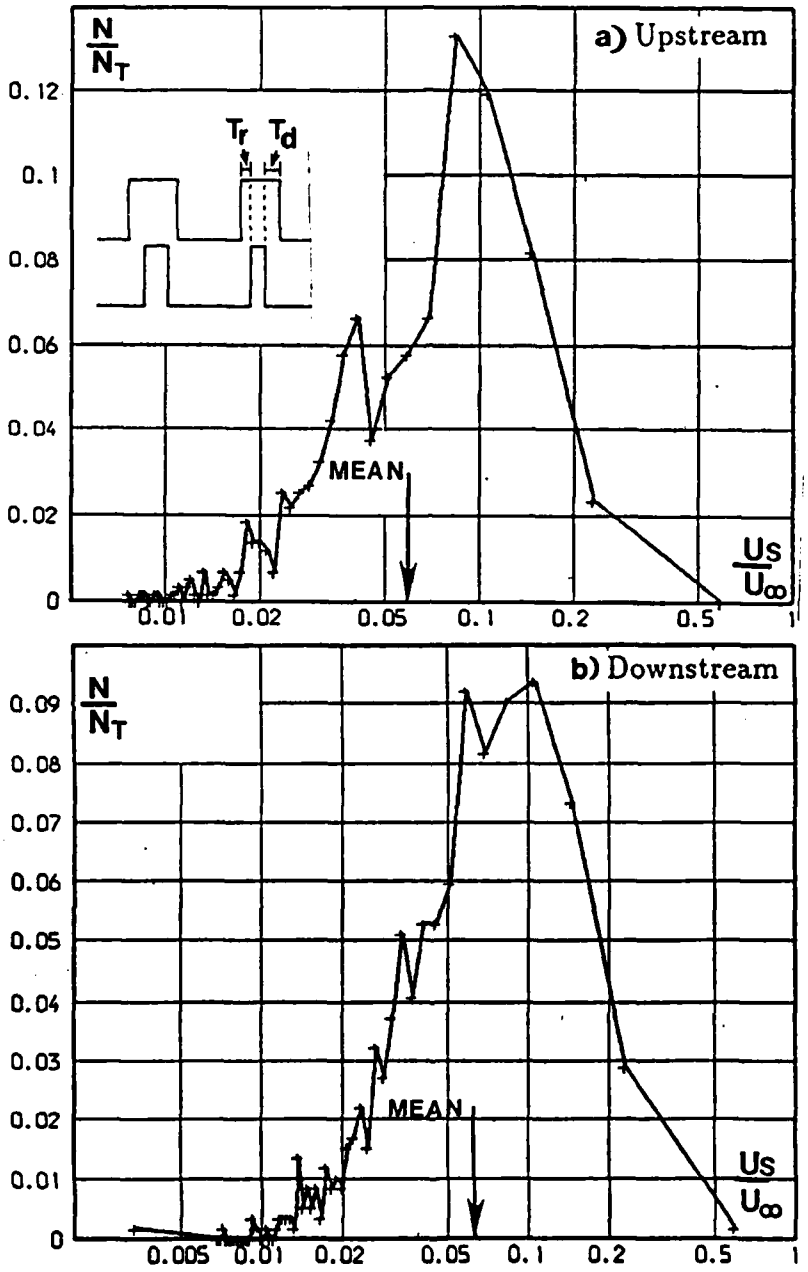

Figure 7. Probability Density Distributions of Shock Speeds in Upstream and Downstream Directions [D = 1.91 cm, Tunnel Floor Boundary Layer]

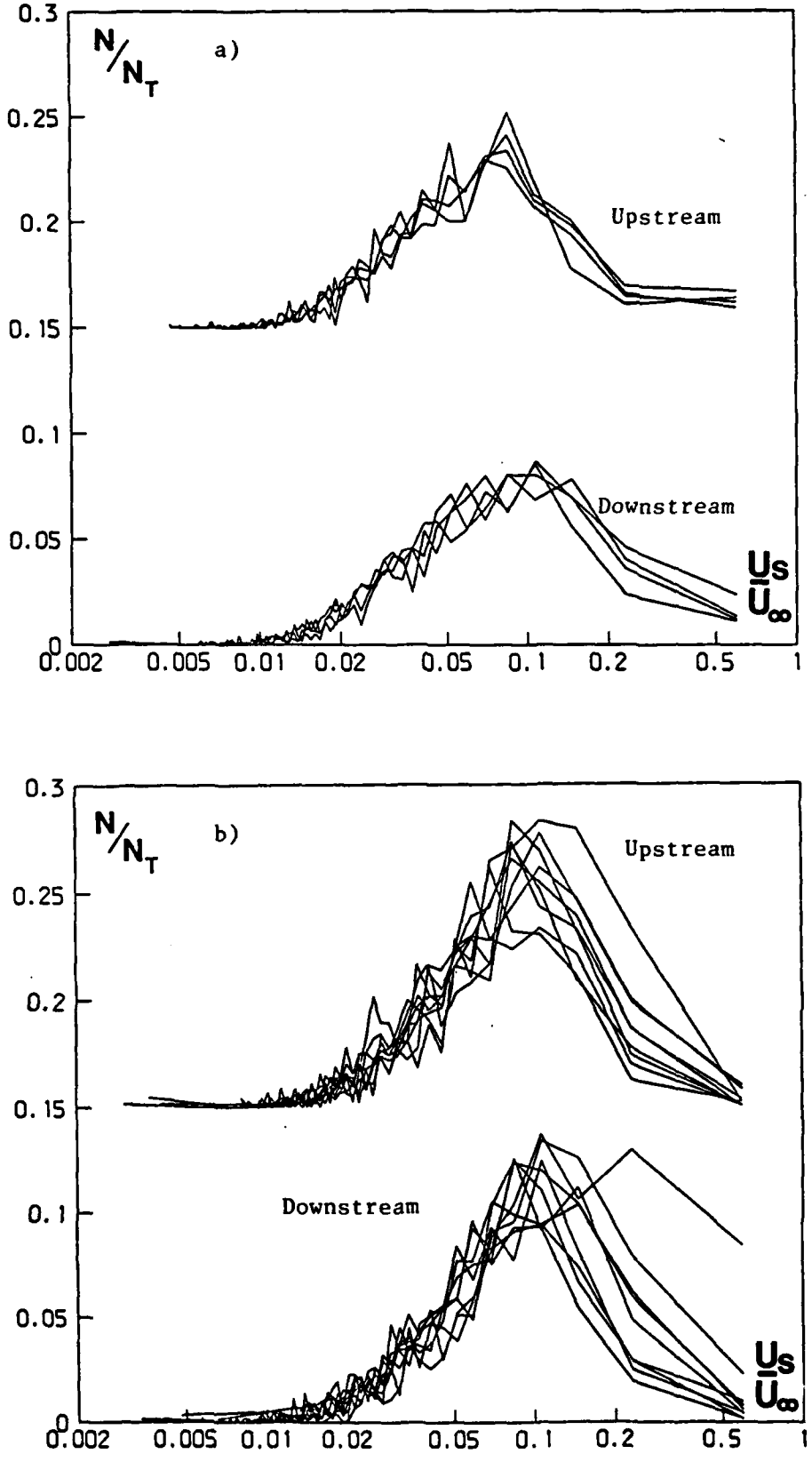

Figure 8. Shock Speeds in Upstream and Downstream Directions in Tunnel Floor Boundary Layer. a) D = 1/2", b) D = 3/4"

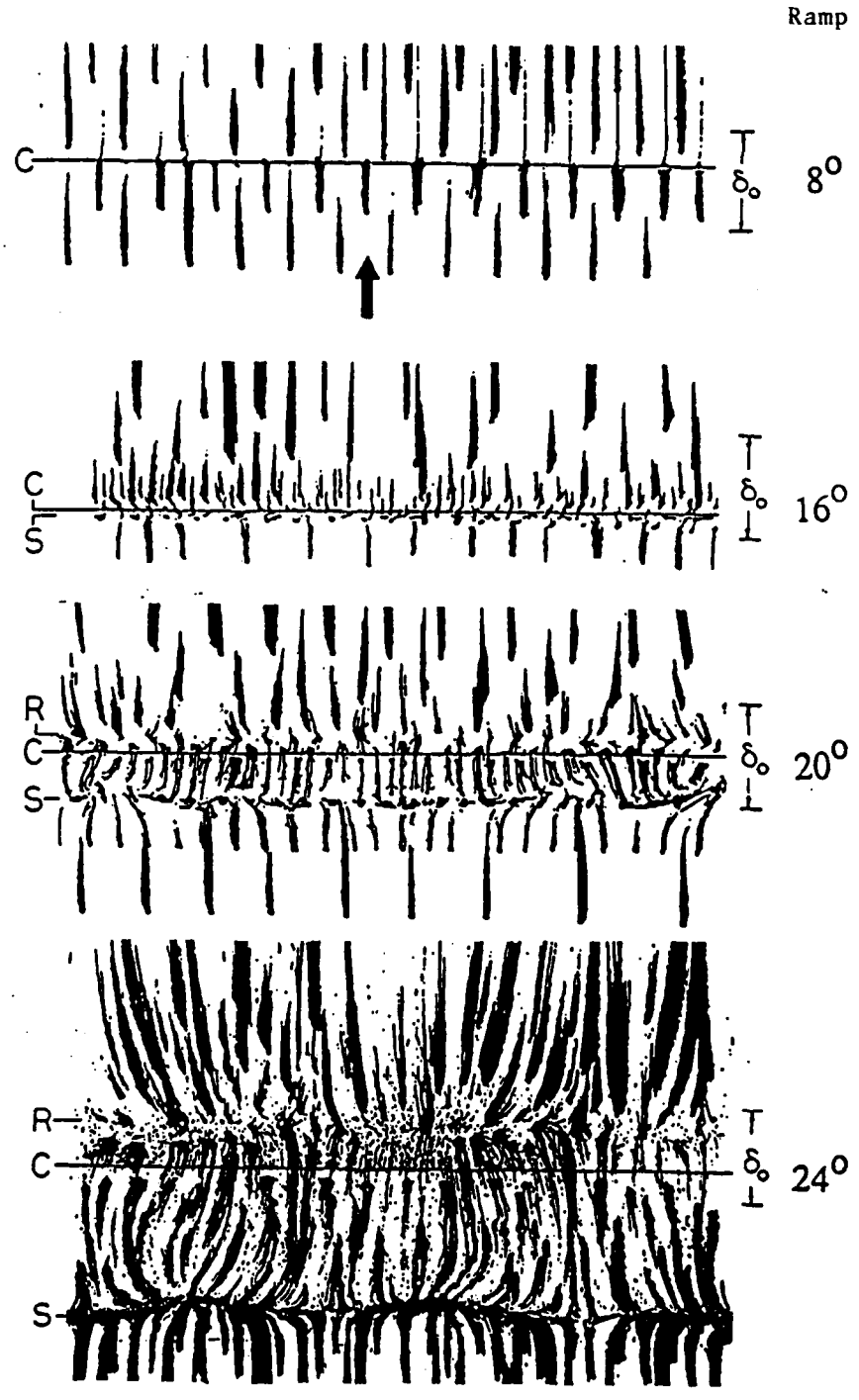

Figure 9. Surface Tracer Patterns (Mach 3, Compression Ramp Flows)

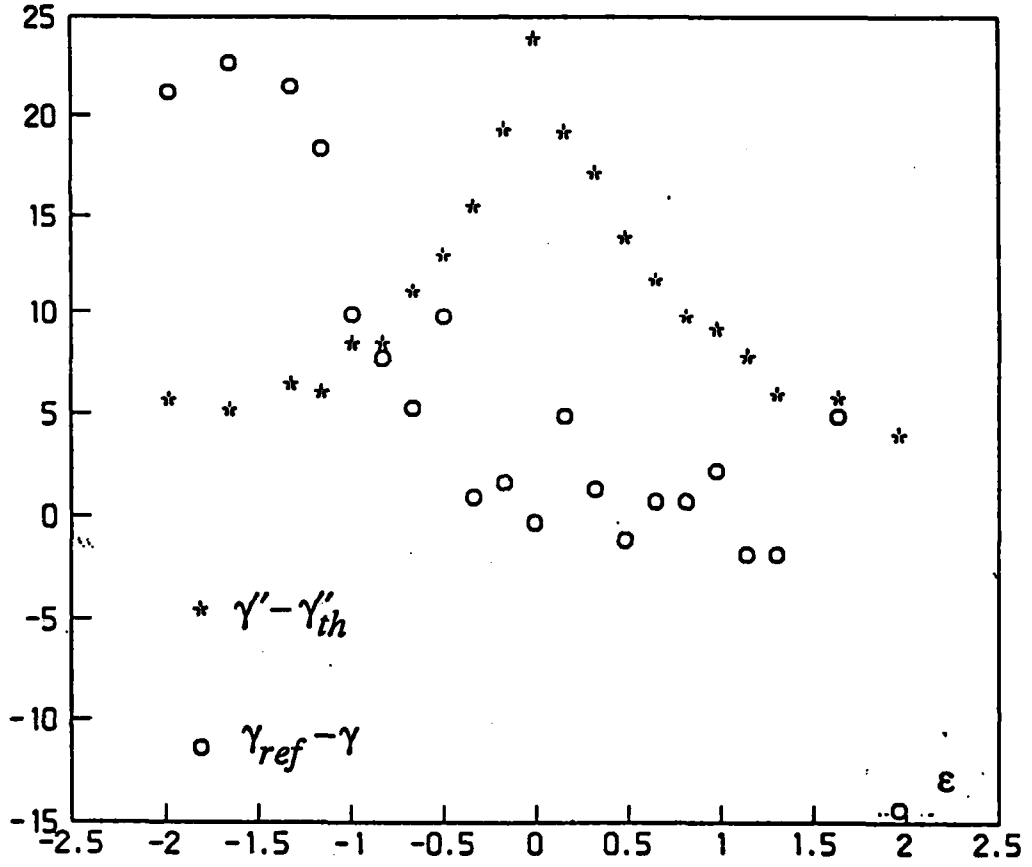

Figure 10. Variation of co-intermittency and intermittency with ε

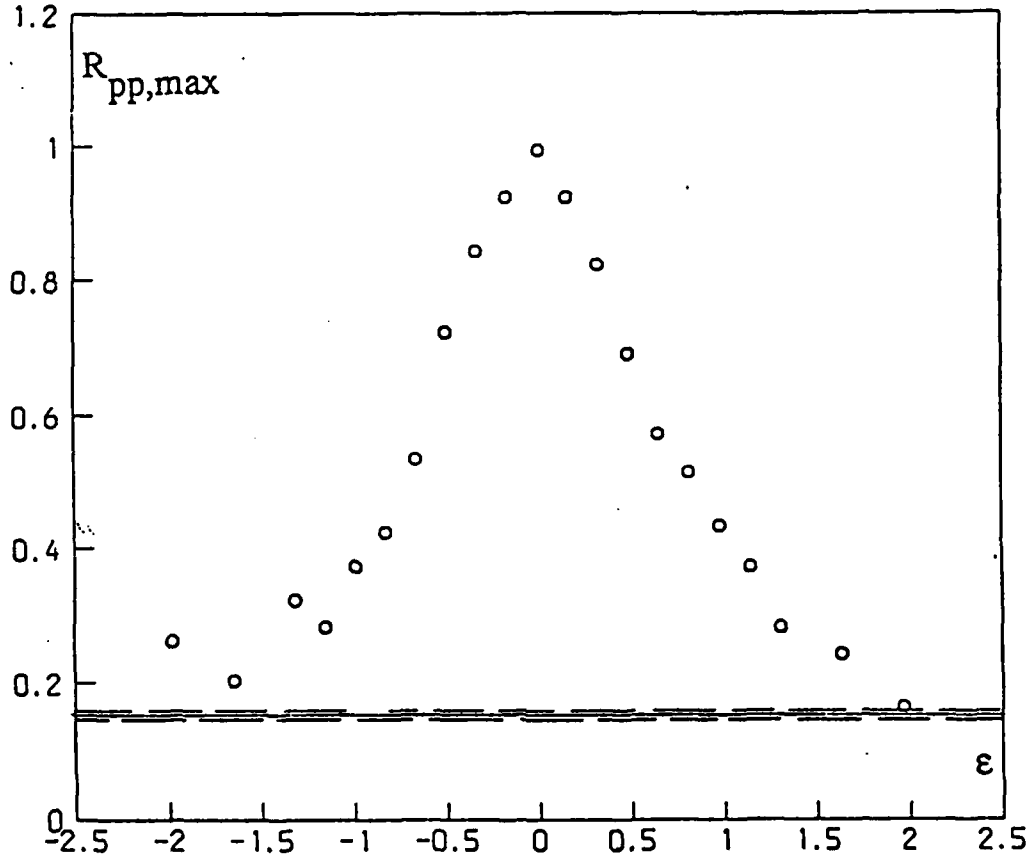

Figure 11. Plot of $R_{pp,max}$ vs. ε

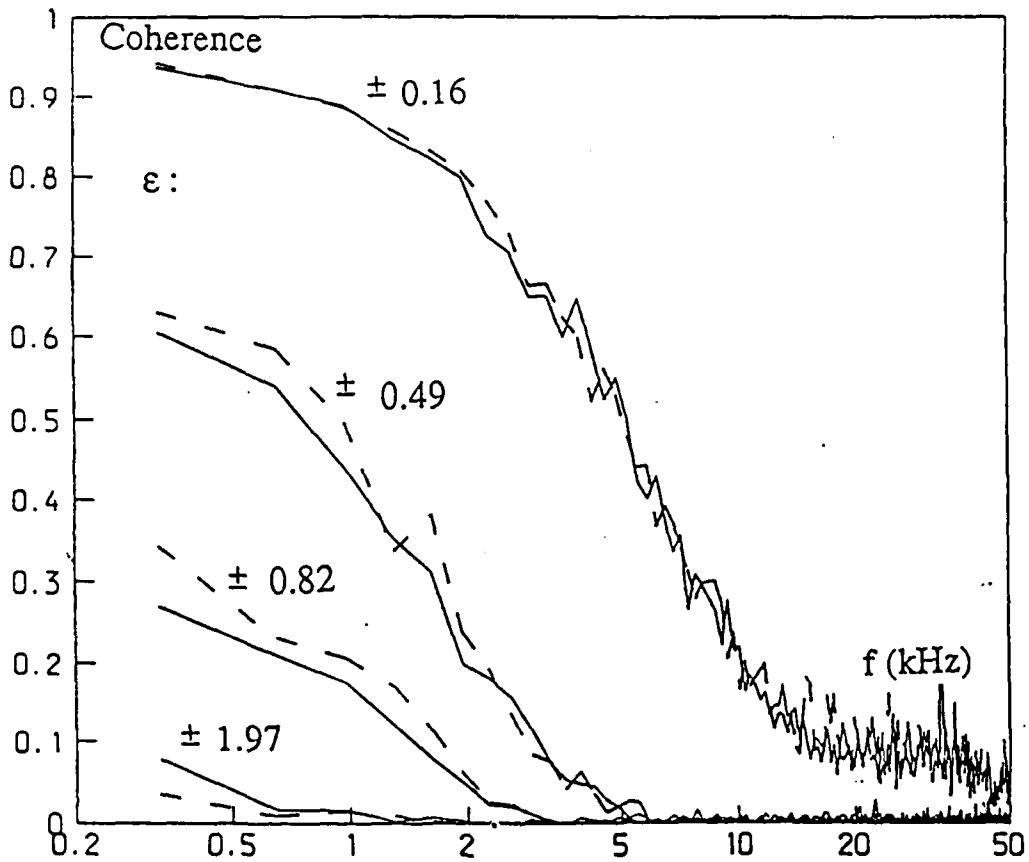

Figure 12. Effect of Lateral Spacing on Coherence Function ($\varepsilon = Z/\delta_o$)

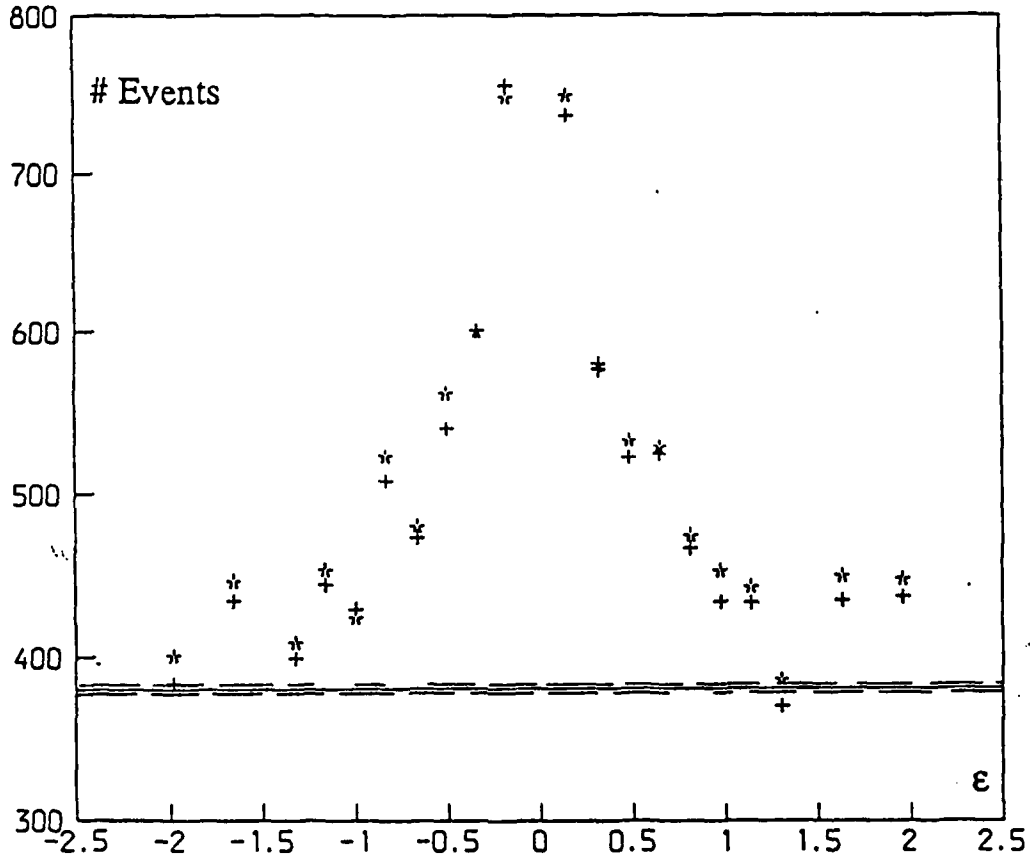

Figure 13. Number of rise and fall events

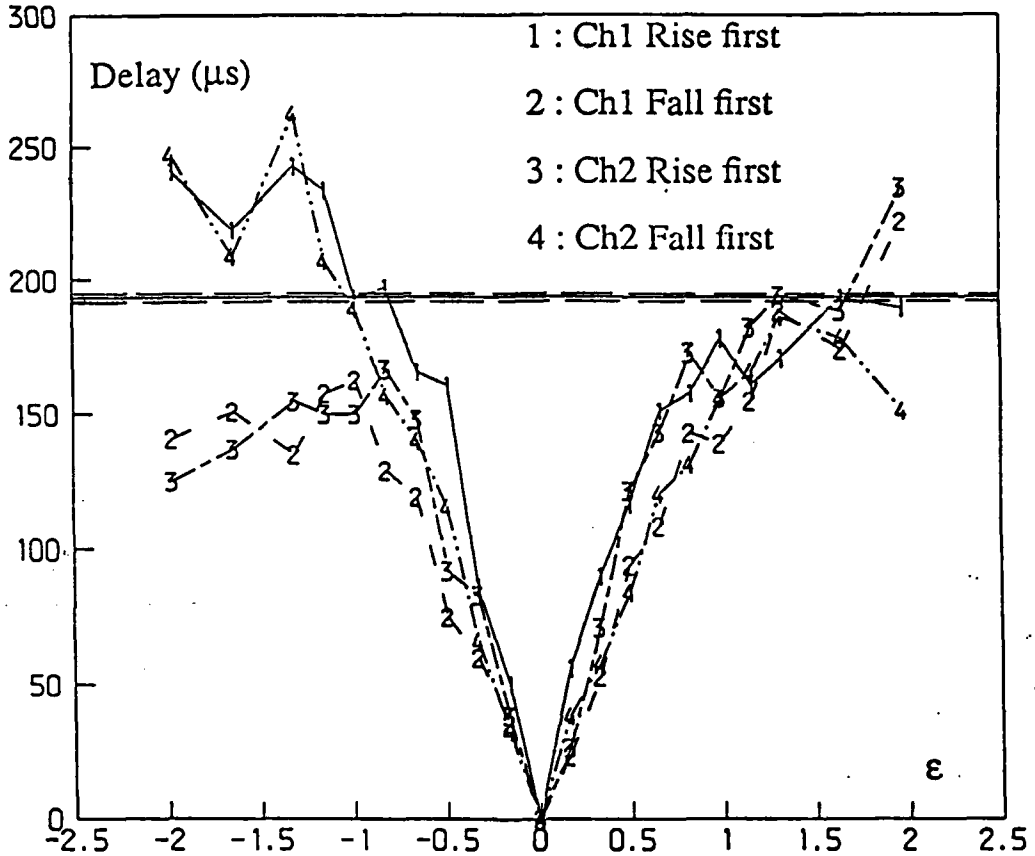

Figure 14. Mean delay times

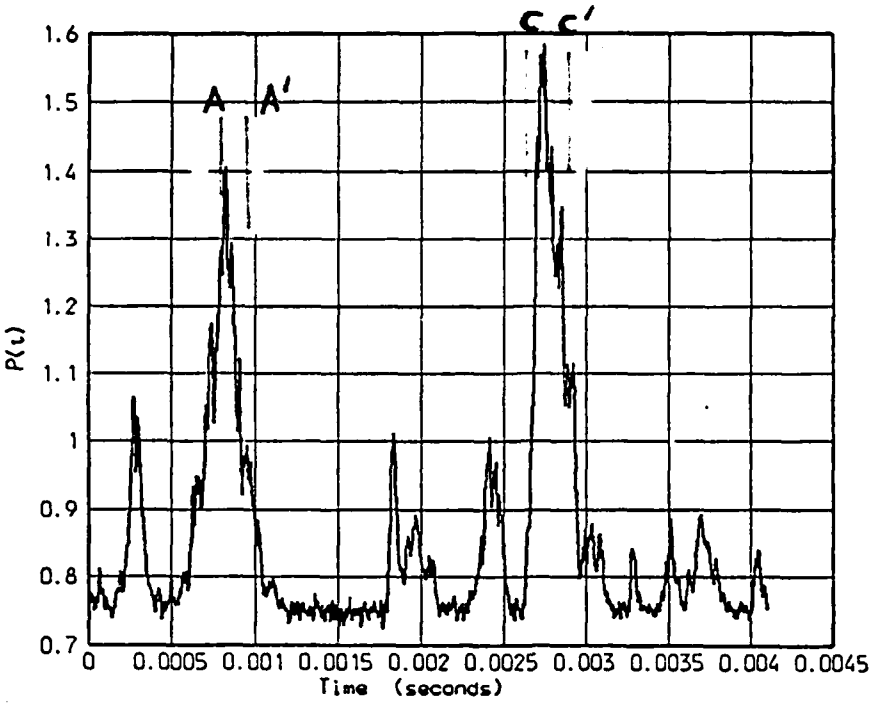

a) Channel 1
(Downstream)

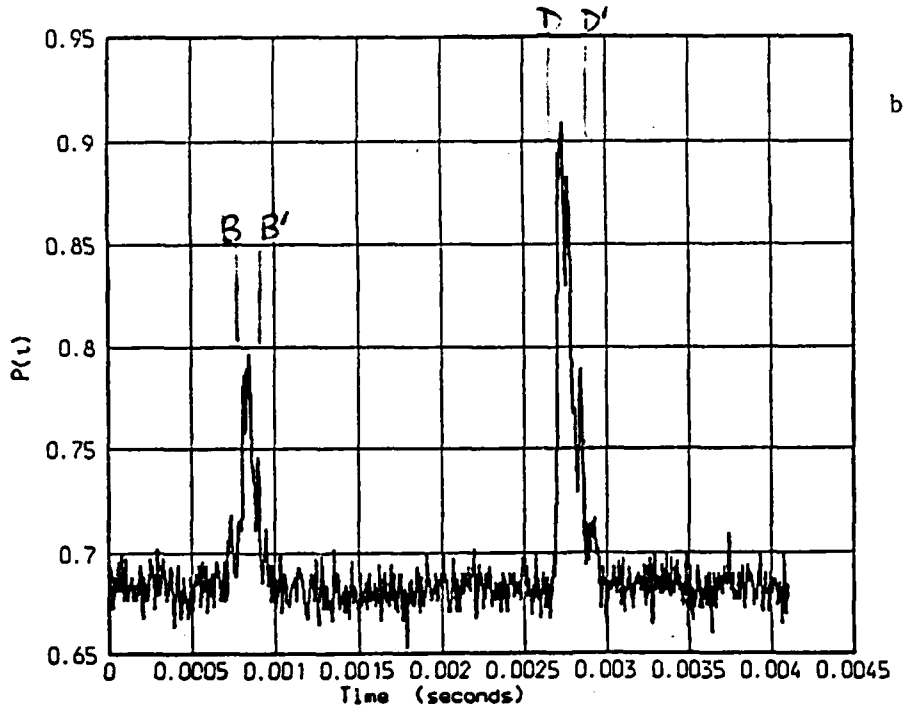

b) Channel 2
(Upstream)

AA' correlated with BB' , CC' correlated with DD', etc.

Figure 15. Cross-Correlation of Components of Pressure Signal Downstream of Moving Shock Wave

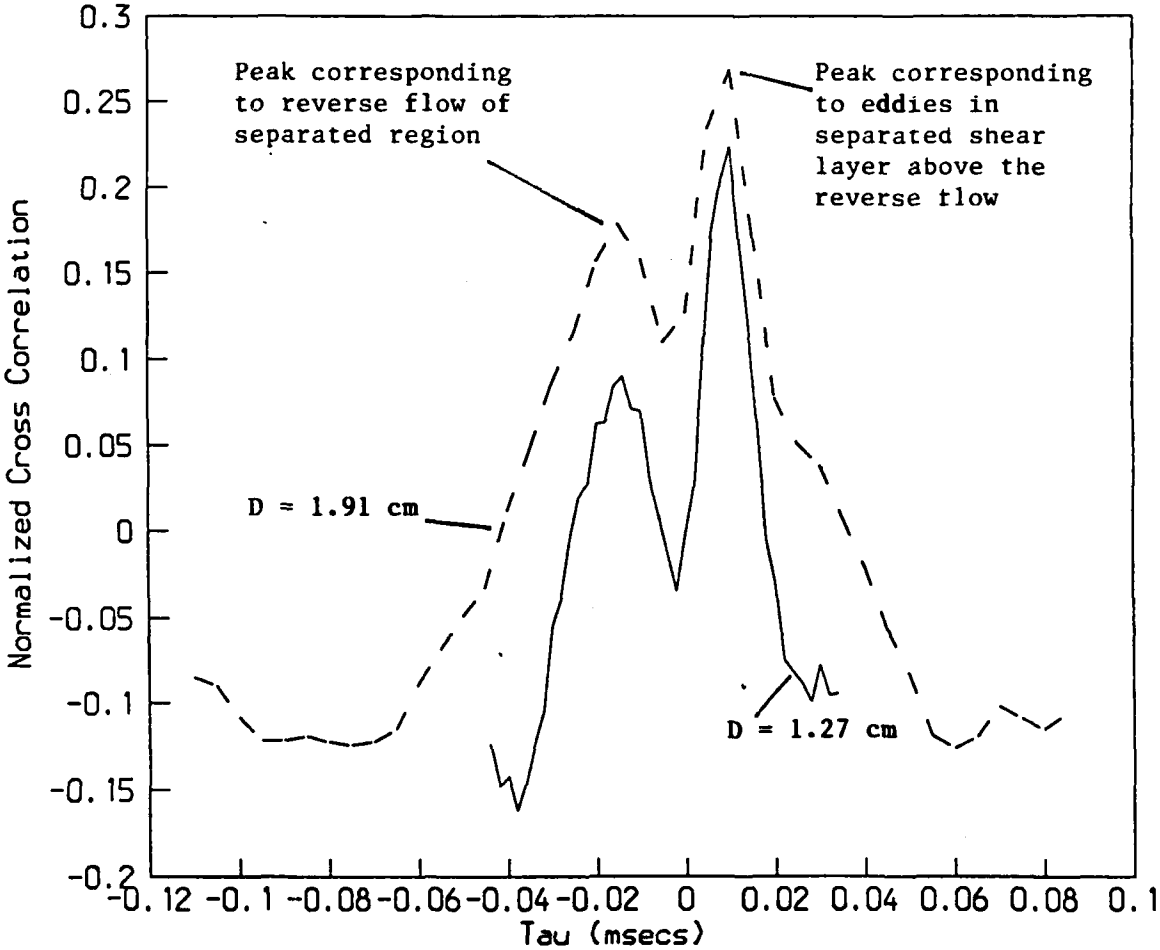

Figure 16. Cross Correlations of Conditionally Sampled Signals of Type Shown in Figure 15.

END

DATE

FILMED

DTIC

JULY 88